Chapter 1

Mechanisms of denitration

1.1 Introduction

The first stage of thermolytic decomposition for nitrate esters is widely considered to be homolytic fission of the O-N bond linking the nitrate to the alkyl chain, leading to the loss of $^{\cdot}NO_2$ (equation 1.1) [1] Though nitrate homolysis is an endothermic reaction, the weak O-N bond has a typical dissociation enthalpy of 42 kcal mol^{-1} and is easily cleaved when exposed to elevated temperatures, UV light or impact. Whilst the thermolytic degradation of energetic materials has been widely studied experimentally, the ambient, slow ageing mechanisms are less well documented. Low-temperature decomposition routes are influenced by many factors over a protracted lifetime, and in practical use, materials are usually subject to evolving environmental conditions. External changes in pressure, humidity, stress and temperature cycles induce variation in the degradation patterns of energetic materials. The presence of moisture has been observed to lower the activation energy and accelerate the decomposition of energetic materials [2]. Internal factors including impurities and residual solvent, and crystal growth within the bulk, also alter decomposition behaviour.

$$R{-}ONO_2 \longrightarrow R{-}O^{\cdot} + {}^{\cdot}NO_2 \tag{1.1}$$

$$R{-}ONO_2 \longrightarrow R{=}O + HNO_2 \tag{1.2}$$

The decomposition of nitrate esters at temperatures over 100°C is dominated by thermolytic processes, whilst under 100°C, decomposition is thought to largely be the result of hydrolysis [3]. Tsyshevsky *et al.* studied the intramolecular reactions leading to denitration in **PETN!** (**PETN!**) in both the vacuum and the bulk crystal [4] (figure 1.1). It was found that the two dominating decomposition reactions were homolysis (equation 1.1) and intramolec-

1. $^{\cdot}NO_2$ loss
2. HNO_2 loss
3. OONO rearrangement
4. γ-attack
5. $ONO_2^{\cdot}$ loss
6. C−C cleavage ($CH_2O + NO_2$)
7. C−C cleavage ($CO + HNO_2$)

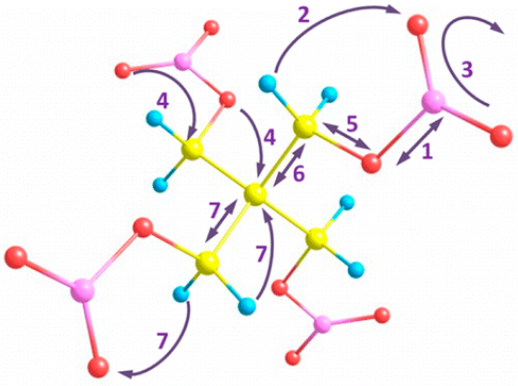

Figure 1.1: Intramolecular thermolytic reactions in **PETN!**, from the work of Tsyshevsky *et al.* [4].

ular elimination of HNO_2 (equation 1.2). Whilst elimination of HNO_2 was found to be the most energetically favourable denitration pathway, homolytic fission dominated preliminary decomposition steps due to the lower activation barrier and faster rate of reaction. It was suggested that global decomposition processes were determined by the interplay between the two mechanisms. Initial homolysis facilitated wide-spread denitration, complemented by exothermic HNO_2 elimination promoting self-heating of the system and further bond dissociations. The presence of $^{\cdot}NO_2$ and HNO_2 were previously linked to autocatalytic rates observed for later-stage decomposition [5, 6, 7]. However, from these initial processes it is not possible to determine which is the species resposible

Spent acids remain in the **NC!** (**NC!**) matrix following synthesis even with thorough washing procedures. Acids are further generated via the subsequent reactions of $^{\cdot}NO_2$ following homolysis. The acidic species proceed to react with other moieties in the system, such as unsubstituted alcohol side chains on the polysaccharide, or other small molecules free in the bulk. When exploring the interaction of nitroglycol and nitroglycerin in acid solution, Camera proposed a protonation-denitration scheme whereby initial protonation at the nitrate is rapid, but subsequent release of the nitronium ion was slow (scheme 1.1).

$$CH_3CH_2ONO_2 + H^+ \overset{\text{fast}}{\rightleftharpoons} CH_3CH_2ONO_2H^+ \tag{1.3}$$

$$CH_3CH_2ONO_2H^+ \overset{\text{slow}}{\rightleftharpoons} CH_3CH_2OH + {NO_2}^+ \tag{1.4}$$

Scheme 1.1: The relative rate of stepwise protonation and denitration of nitrate esters, using ethyl nitrate as an example. From the work of Camera *et al.* [8].

NC! in storage is kept wetted with solvents to prevent drying and self-ignition. Material with 12.6**pN!** or lower, must be stored in 25% water by mass, or a mixture of solvents and plasticisers. In the study of organonitrates and organosulfates generated from isoprene as secondary organic aerosols, Hu *et al.* found that primary and secondary nitrates were resilient to hydrolysis for pH > 0, whilst tertiary nitrates underwent hydrolytic nucleophilic substitution easily, reacting with water to form alcohols [9]. Primary nitrates are those with

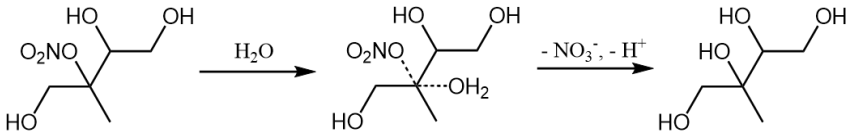

Scheme 1.2: Hydrolysis of a tertiary nitrate derived from the reaction of isoprene in the aerosol phase, from the work of Hu *et al.* [9].

one non-hydrogen moiety on the carbon, (additional to the nitrate linkage) with the remaining two bonds linked to hydrogens. Secondary nitrates are those where the nitrate carbon posses one bonded hydrogen atom, and two further non-hydrogen moieties. In tertiary nitrates, the carbon is fully substituted with no attached hydrogens. This latter group is usually sterically hindered and stabilising to carbocations, condition on the other substituents. If formation of a carbocation intermediate is involved in the hydrolysis mechanism, this may explain why the tertiary nitrates exhibited highly efficient denitration, even under neutral conditions.

Though no specific mechanistic detail is given, the action of a protonated transition state during hydrolysis is alluded to by Hu *et al.*, through the contrast between the rate of acid-catalysed and neutral hydrolysis reactions. Neutral hydrolysis of the tertiary nitrates occured rapidly, but hydrolysis only occurred for primary and secondary nitrates under strongly acid catalysing conditions at much lower rate. It was found that the presence of adjacent OH groups hampered the rate of hydrolyis for some aerosol dispersed organonitrates. In the neutral hydrolysis of tertiary nitrates, increasing the number of adjacent OH groups lead to protracted hydrolysis lifetimes. Interestingly, the retardation effect of adjacent OH groups was not observed for the the acid catalysed cases. Hu proposed that this could be due to the interaction of OH with the transition state of the neutral hydrolysis system, compared to the protonated transition state of the acid catalysed system, impeding the reaction only in the former case. There is evidence that nitration and denitration of nitrate esters is also influenced by the presence of nitrate groups at neighbouring positions.

Matveev *et al.* demonstrated that for poly-nitroesters the rate of liquid-phase decomposition did not increase linearly with number of nitrate reaction centres. It was found to mainly dependend on individual structures (table 1.3) [10].

It was suggested that the trend in reactivity could be partially explained by the inductive effect of the nitro groups [1]. The inductive effect arises when a difference in the electronegativity between atoms connected by a σ bond leads to a polarisation, or permanent dipole, in the bond. Electron donating groups increase the δ- partial charge on neighbouring atoms through the release of electrons, whilst electron withdrawing groups pull electron density away from neighbouring atoms generating a δ+ charge on connected atoms. However, the π donation by lone pairs on the oxygen and nitrogen plays a significant role in increasing electron density of neighbouring atoms, known as the resonance effect. NO_3 presents a stronger electron donating effect via π donation than OH. It would therefore be expected that both increase the rate of hydrolysis for nearby leaving groups. The presence of an adjacent nitrate appears to facilitate denitration, whereas the presence of hydroxyl groups hinders this process, for neutral hydrolytic schemes. This suggests that the proposed interaction of the hydroxyl group with the neutral transition state supersedes its resonance effect. As a result, it is ambiguous whether any apparent rate increase due to the presence of adjacent nitrate groups arises as a result of the resonance effect of the nitrate, or whether it is solely due to the absence of a neighbouring hydroxyl.

Table 1.1: Comparison of rate constants of decomposition for various polynitrate esters at 140°C. Collated from literature sources by Matveev *et al.*[10]. ΔT is the decomposition temperature range, E is the experimental activation barrier for decomposition, log$A$ is the pre-exponential factor, T_c is the combustion temperature, k_{expt} is the rate constant for decomposition.

Compound	ΔT / °C	E / kcal mol^{-1}	log$A$ [s^{-1}]	k_{expt} / 10^{-6} s^{-1}
$O_2NOCH_2CH_2CH_2ONO_2$	72–140	39.1	14.9	1.7
$O_2NOCH_2CH_2CH_2CH_2ONO_2$	100–140	39.0	14.7	1.1
$O_2NOCH(CH_3)CH(CH_3)ONO_2$	72–140	40.3	14.9	5.0
$O_2NOCH_2CH_2OCH_2CH_2ONO_2$	80–140	42.0	16.5	1.9
$O_2NOCH_2CH(OH)(CH_2ONO_2)$	80–140	42.4	16.8	2.3
$O_2NOCH_2CH(ONO_2)(CH_3)$	72–140	40.3	15.8	3.0
$[(O_2NOCH_2)CH(ONO_2)CH(ONO_2)]_2$ (hexanitromannite)	80–140	38.0	15.9	63.0

The investigation by Hu *et al.* exclusively focused on nitrates generated from an isoprene precursor, upon dispersion as an aerosol. The nitrate groups present in **NC!** are either of primary (C6) or secondary (C2, C3) structure, indicating that ambient hydrolysis is unlikely according to this scheme. However, solvent effects are expected to differ for condensed-phase reactions and aerosol phases. A greater build-up of acid concentration can be achieved in a closed, condensed system, and the lifetime of an aerosol is relatively short-lived when considering the timescale of slow ageing processes in **NC!**. Thus, the work of Hu *et al.* does not provide a direct comparison for the **NC!** polymer but highlights the the possible contribution from both neutral and acid-catalysed hydrolysis routes and of increasing levels of substitution on the wider structure.

In this section, the possible mechanisms for nitrate removal from the **NC!** backbone are explored. The homolytic fission and HNO_2 elimination thermolytic processes suggested by Tsyshevsky will be compared to the acid hydrolysis scheme. Though the relative rates of reaction were not compared, the extended timescales involved in ambient ageing imply that the dominating reactions correspond to those most thermodynamically favourable.

1.2 Methodology

The energies of homolytic fission and elimination of HNO_2 were calculated for PETN, as a test system before extension to the monomer. The reaction energies were calculated according to equations 1.1 and 1.2 to reproduce the work of Tsyshevsky *et al.*. The literature geometries of PETN and its derivatives were obtained from the authors. A single point energy and frequency calculation were performed on each of the relevant structures to determine the reaction energies; no geometry optimisation was performed on the given structures except for in the case the $^{\cdot}NO_2$ molecule, where the geometry was not given.

The intramolecular reactions of the **NC!** monomer were modelled according to scheme 1.3. Rigid and relaxed **PES!** (**PES!**) scans were attempted in order to locate transition states for both reactions for the **NC!** monomer. Where the scans were unable to identify a valid transition state geometry, guess transition state geometries were constructed and optimised.

The possible protonation sites for the **NC!** monomer were explored by placing a proton at each of the different oxygen sites surrounding the nitrate group. The structures were then geometry optimised and energies of protonation were compared. H_3O^+ was modelled as the donating species; as **NC!** is usually stored wetted in water, the hydronium ion is the most likely source of protons. It is also possible that the proton is donated by other acidic species

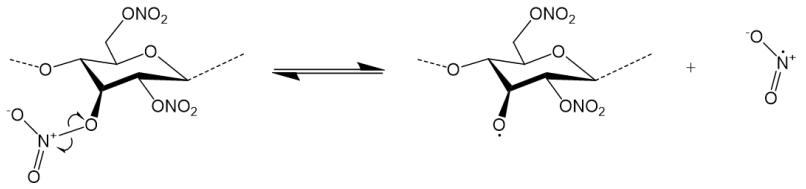

(a) Removal of a nitrate group *via* homolytic fission of **NC!**

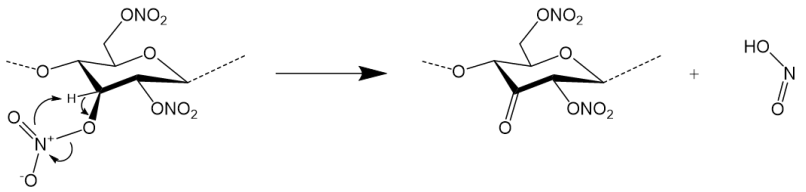

(b) Removal of a nitrate group *via* elimination of HNO_2.

Scheme 1.3: The proposed intramolecular reactions for the initial denitration step during **NC!** degradation.

in the system, particularly HNO_2 or HNO_3. This is more likely at later stages of degradation when a higher concentration of acid has been generated by secondary reactions.The effects of tunneling were not accounted for.

1.2.1 Computational details

All geometry optimisation, thermochemistry calculations and **PES!** scans were performed in **G09!** (**G09!**). Geometry optimisation and thermal calculations were to the level of 6-31+G(2df,p). **NC!** monomer structures were optimised using **wb97xd!** (**wb97xd!**), **B3LYP!** (**B3LYP!**) and **MP2!** (**MP2!**). ΔG values were obtained by the difference between the thermally corrected free energies of products and reactants. Zero-point corrected energies **ZPE!** were determined by addition of individual **ZPE!** (**ZPE!**) to the free energy:

$$\Delta G^{ZPE} = \sum(G_{products} + ZPE_{products}) - \sum(G_{reactants} + ZPE_{reactants}) \tag{1.5}$$

PES! scans were performed to the level of **wb97xd!**/6-31+g(d), or using unrestricted **wb97xd!**, in the case of O$-$'NO_2 dissociation. Rigid scans were carried out by fixing bond lengths, angles and dihedral values as constants. Only the variable of interest was allowed to change, with the exception of relaxation of other specified coordinates required for accommodation of the new geometry, following each step of the scan. For example, in the homolysis of the nitrate O$-NO_2$ bond, as the NO_2 group departed, the internal O–N–O angle was also allowed to relax, in addition to the angle of the departing NO_2 with respect to the remainder of the molecule. In two-dimensional scans, two variables are scanned. For

the same reaction, the elongation of a the O−NO_2 bond was scanned with simultaneous approach of a proton, to monitor the effect of protonation for the same reaction. Relaxed scans were performed in Gaussian using the ‘modredundant‘ function, whereby the whole structure was geometry optimised after each step of the scan. Scans were performed with step size of 0.1 Å. The number of steps varied with the property investigated, though the majority of the phenomena were observed within 20 steps (2 Å). Scans were attempted in vacuum, and for some cases, **PCM!** (**PCM!**) implicit solvent [11].

1.3 Results and discussion

1.3.1 Thermolytic decomposition mechanisms

The energies of homolytic fission and intramolecular elimination of HNO_2 from a **PETN!** nitrate group are shown in table 1.2. The energy values calculated by Tsyshevsky *et al.* are denoted in parenthesis. Despite using the supplied geometries, same method and basis, it can be seen that the reaction energies obtained for PETN vary greatly from the values found by Tsyshevsky *et al.*. Inspection of the forces showed that they were in fact not converged. It was expected that the given geometries were used to generate the reaction energy values quoted in the study. The unconverged structures therefore do not fully explain the large discrepancy between the literature energies and obtained values here. A small contribution may arise from a different compilation of the **G09!** program, leading to fluctuations in the exact values obtained which are amplified when deriving reaction energies.

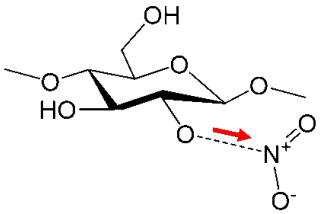

Figure 1.2: The O−NO_2 bond was elongated during rigid and relaxed **PES!** scan to simulate homolytic fission for the **NC!** monomer.

what scans did I do for HNO2? Get a pic of the transistion state.

The energy profile of homlytic fission was obtained via **PES!** scans of NO_2 leaving the **NC!** monomer. The internal angle of the departing NO_2, in addition to the coordinates referencing its orientation relative to the rest of the molecule, was allowed to relax. As the scan progressed the NO_2 internal angle increased from 129.2 °to 134.0 °at a maximum separation of 3.4 Åfrom the bridging oxygen (Ox), corresponding to the formation of a

Table 1.2: Calculated free energies of reaction (ΔG_r), reaction enthalpies (ΔH_r), activation barriers (E_a) with zero-point correction (^{ZPE}) for the intramolecular reactions of PETN, and the **NC!** monomer. Values expressed in kCal mol^{-1}.

Reaction	ΔG_r	ΔG_r^{ZPE}	ΔH_r	E_a	$E_a{}^{ZPE}$
PETN					
$^{\cdot}NO_2$ loss	21.51 (41.2)[a]	16.56 (35.8)	35.62	21.51[b] (41.2)	16.56 (35.8)
HNO_2 loss	−23.63 (−18.6)	−26.21	−20.39	41.29 (47.3)	36.28 (42.7)
NC! monomer					
$^{\cdot}NO_2$ loss	23.25	18.69	36.26	23.25	18.69
HNO_2 loss	−36.05	−39.42	−22.86	40.70	37.33

[a] values from the work of Tsyshevsky *et al.* [4].
[b] values for the activation energy and total energy of reaction are the same for bond dissociation via homolytic fission.

$^{\cdot}NO_2$ radical (internal angle 134.3 °).

1.3.2 Acid hydrolysis mechanism

1.3.2.1 Protonation site

The protonated **NC!** monomer species are shown in figure 1.3. The bridging oxygen (Ox) linking the nitrate to the remainder of the molecule, the capping group oxygen, and the interchangeable terminal nitrate oxygen sites were protonated in order to compare their relative energies for determination the site most likely to stabilise the proton at thermal equilibrium. Protonation also occurs on other sites in the molecule, such as at unsubstituted hydroxyl groups, the capping group oxygen on C4 and O1 in the glucose ring. Though is a possibility that protonation at further sites in the monomer would contribute to degradation processes *via* alternative mechanisms, for the purposes of studying denitration via acid hydrolysis, only the sites peripheral to the nitrate leaving group were explored. The mechanism of protonation was not explored in depth here; it was assumed that the protons in the system would be in fast exchange between the molecule and the solvent. The process has been studied computationally by Jebber *et al.* and Liu *et al.* [**?**, **?**]. The optimisation of water as a protonating species was attempted, to see whether it was possible to stabilise in coordination. The optimisation of H3O in coord with fully nitrated monomer was also tested, but was only possible up to the level hf/6-31g. Evaluation of the energy of protona-

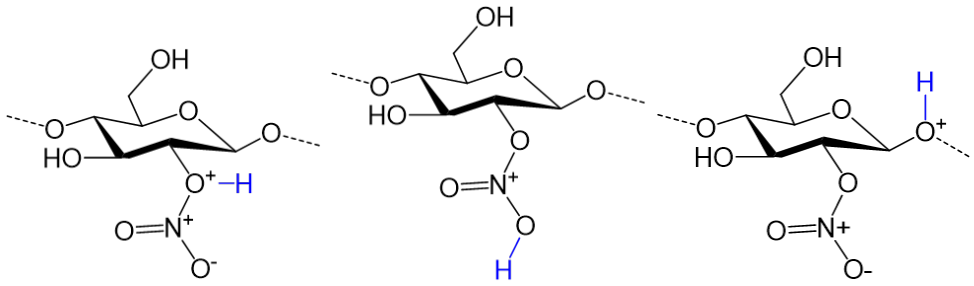

Figure 1.3: Protonation sites on the **NC!** monomer for hydrolysis of the nitrate at the C2 position.

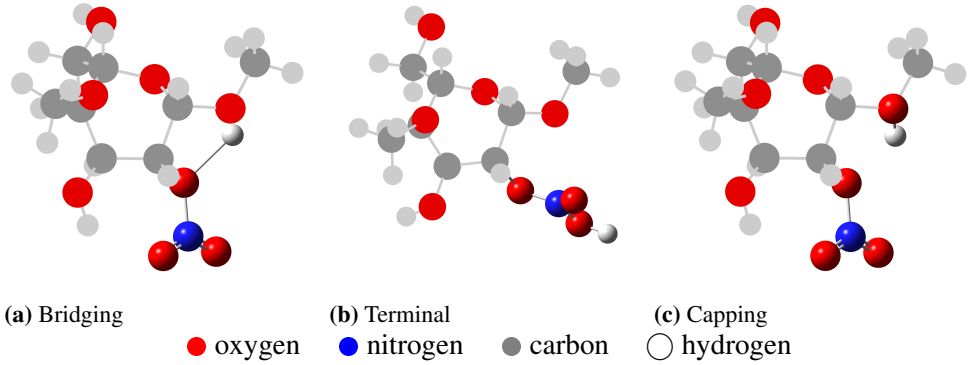

Figure 1.4: Optimised protonated **NC!** monomer structures, showing interaction between the proton on the bridging site with the capping group oxygen.

tion at each site found that the bridging

Big table of all the scans I did (for hydrolysis TS)

Columns:

Scanned co-ordinate. Distance scanned. Observation. (TS found? etc)

1.3.3 Denitration by hydrolysis

Following the protonation step, possible transition states for the removal of the nitrate were investigated. A **PES!** scan was performed on the **NC!** monomer protonated at the bridging

Table 1.3: Free energies of protonation at each of the oxygen sites of interest on **CH3CH3!** (**CH3CH3!**) C2 monomer of **NC!**.

Protonation site	ΔG_r /kcal mol^{-1}			
	wb97xd!	PCM	**B3LYP!**	PCM
Bridging	−30.88	0.85	−31.99	−0.25
Terminal	−23.13	10.00	−24.06	10.97
Capping	−30.43	0.85	−31.98	0.64

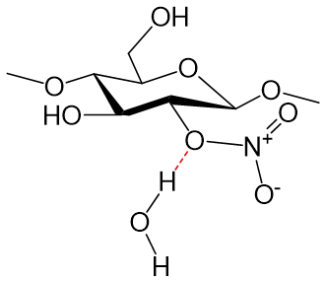

site, where the O−NO_2 bond was elongated in order to determine whether the NO_2 is lost, leaving the hydroxyl group as expected. Unrestricted **wb97xd!** was used, with 20 steps of 0.1 Å, however bond dissociation was not observed even when extending the scan distance to a maximum of 6.4 Å. Instead, a steady increase in the energy was observed.

The **PES!** scan of NO_2 removal from ethyl nitrate protonated at the bridging site was used as a preliminary test for the mechanism of denitration following protonation. 4-membered ring and 6-membered ring structures were optimised in order to determine

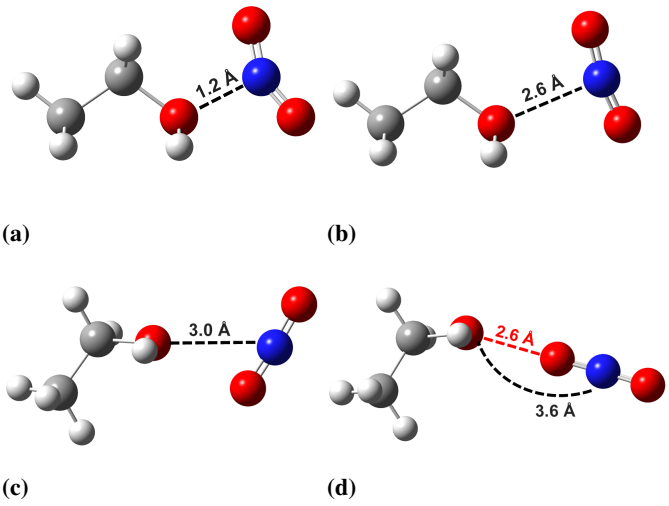

whether they were energetically and geometrically feasible. It can be seen that as the nitrate departs, it aligns with the hydroxyl group in an orientation suitable for formation of a peroxy group. Optimisations were attempted with both full geometry relaxation, and various frozen co-ordiate schemes; fixing of the bulk molecule with relaxation only around the nitrate and co-ordinating species or relaxation of the wider molecule with fixed coordinates around the nitrate. Fully relaxed structures did not show convergence. It was possible to optimise the 4-membered ring bridging transition state with frozen ring geometry and relaxation of the remaining molecule (figure 1.6b). A rigid scan of the 4-membered ring transition starting from the bridging protonation site revealed that as the nitrate moved away from the system,

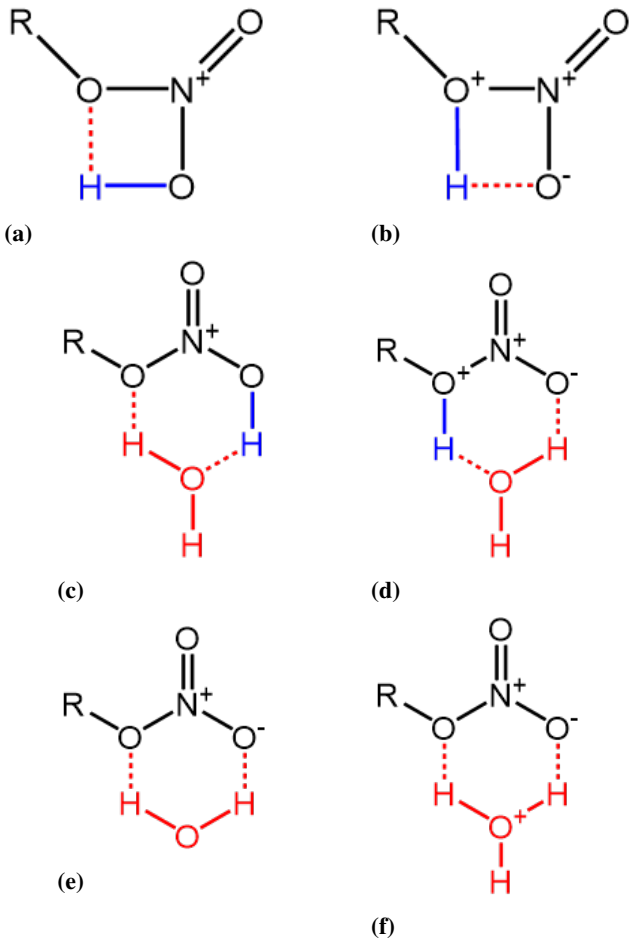

Figure 1.6: Proposed 4-member and 6-member ring transition states for the denitration of a nitrate ester, under various hydrolytic conditions. R = CH_3 in the case of methyl nitrate, R = CH_2CH_3 in the case of ethyl nitrate and R = $(H_3CO)_2C_6H_9O_3$ for the monomer.

the proton moved to the capping group site rather than remain on the bridging oxygen as a hydroxyl, as was expected. Instead a ketone group was formed between the bridging oxygen and the ring. At subsequent steps, the ketone group causes the C2 - C3 bond to elongate and break. The scan eventually revealed the NO_2 leaving group reclaiming the proton from the capping group oxygen, leading to ring fission.

Things I did:

4 membered ring

–Scan using ethyl nitrate

–Opt Ts using ethyl nitrate

–considerations - sterics, and what energy barrier would be required to overcome the twist needed to obtain this state. Orbital overlaps?

6 membered ring

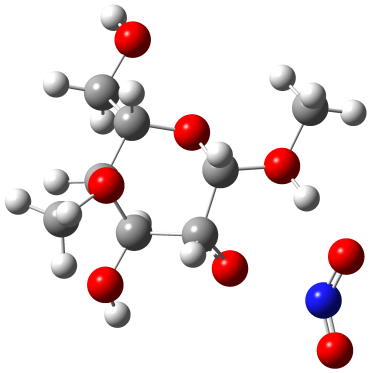

(a) In the initial stages of increasing O−NO_2 distace, the proton moves to the capping group.

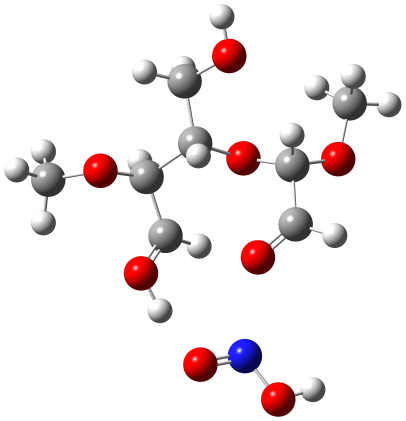

(b) At separation of over 3.3 Å, the bond between C2 an C3 breaks, leading to ring fission. The proton then eventually moves back onto NO_2 .

Figure 1.7: Relaxed scan of NO_2 departure, starting with the 4-membered ring structure.

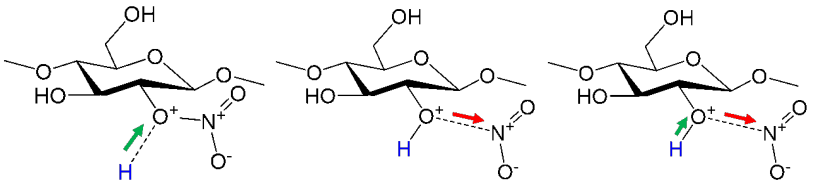

Figure 1.8: The scanned coordinates.

–considerations - sterics, and what energy barrier would be required to overcome the twist needed to obtain this state. Orbital overlaps?]

–Would energetics allow you to skip the protonation step? Is it more favourable?

C2 and water

1.4 Summary

Homolysis is fastest, for the monomer too, with HNO2 coming in second due to slower rate / energetics. (Check if I did anything to actually find this out - may just have to compare energetics.) Scans did confirm that ˙NO_2 left as a radical. Scans showed the energy profiles involved (again, was HNO2 ever seen to be formed?)

AH rate was not able to be compared as a TS was not found. Protonation occurs on both terminal and bridging sites of the monomer, with location at the bridging site conducive to the removal of NO_2^+.

TS were not able to be isolated for the denitration step, even with coordination with

water in different orientation and both 4 and 6 mem ring TS. 2D scans did reveal a possible TS but it did not lead to the desired denitration pathway.

Bibliography

[1] Jimmie C. Oxley. A survey of the thermal stability of energetic materials, jan 2003.

[2] M F Foltz. Aging of pentaerythritol tetranitrate (PETN). *LLNL-TR-415057, Lawrence Livermore National Laboratory, Livermore, CA, USA*, apr 2009.

[3] Mohammed Moniruzzaman, John M. Bellerby, and Manfred A. Bohn. Activation energies for the decomposition of nitrate ester groups at the anhydroglucopyranose ring positions C2, C3 and C6 of nitrocellulose using the nitration of a dye as probe. *Polymer Degradation and Stability*, 102:49–58, apr 2014.

[4] Roman V. Tsyshevsky, Onise Sharia, and Maija M. Kuklja. Thermal Decomposition Mechanisms of Nitroesters: Ab Initio Modeling of Pentaerythritol Tetranitrate. *The Journal of Physical Chemistry C*, 117(35):18144–18153, sep 2013.

[5] I. Rodger and J. D. Mcirvine. The decomposition of spent PETN nitration acids. *The Canadian Journal of Chemical Engineering*, 41(2):87–90, apr 1963.

[6] Torbjórn Lindblom. Reactions in stabilizer and between stabilizer and nitrocellulose in propellants. *Propellants, Explosives, Pyrotechnics*, 27(4):197–208, sep 2002.

[7] Hermann N. Volltrauer and Arthur Fontijn. Low-temperature pyrolysis studies by chemiluminescence techniques real-time nitrocellulose and PBX 9404 decomposition. *Combustion and Flame*, 41:313–324, jan 1981.

[8] E. Camera, G. Modena, and B. Zotti. On the Behaviour of Nitrate Esters in Acid Solution. II. Hydrolysis and oxidation of nitroglycol and nitroglycerin. *Propellants, Explosives, Pyrotechnics*, 7(3):66–69, jun 1982.

[9] K. S. Hu, A. I. Darer, and M. J. Elrod. Thermodynamics and kinetics of the hydrolysis of atmospherically relevant organonitrates and organosulfates. *Atmospheric Chemistry and Physics*, 11(16):8307–8320, aug 2011.

[10] V. G. Matveev and G. M. Nazin. Stepwise Degradation of Polyfunctional Compounds. *Kinetics and Catalysis*, 44(6):735–739, nov 2003.

[11] S. Miertuš, E. Scrocco, and J. Tomasi. Electrostatic interaction of a solute with a continuum. A direct utilizaion of AB initio molecular potentials for the prevision of solvent effects. *Chemical Physics*, 55(1):117–129, feb 1981.